Supporting Information for

$Ba_8SrPb_{24}O_{24}Cl_{18}$: The First Alkali-Earth Metal Lead (II) Oxyhalide with Intriguing Multimember−Ring Layer

Zhuang Li,[a,b,c] Shengzi Zhang,[a,c] Wenhao Xing,[a,b,c] Zheshuai Lin,[a] Jiyong Yao,*[a,b] Yicheng Wu[a,d]

[a] Beijing Center for Crystal Research and Development, Key Lab of Functional Crystals and Laser Technology, Technical Institute of Physics and Chemistry, Chinese Academy of Sciences, Beijing 100190, P. R. China, corresponding author: Jiyong Yao, E−mail: jyao@mail.ipc.ac.cn.

[b] Center of Materials Science and Optoelectronics Engineering， University of Chinese Academy of Sciences, Beijing 100049, P. R. China

[c] University of Chinese Academy of Sciences, Beijing 100049, P. R. China.

[d] Institute of Functional Crystal Materials, Tianjin University of Technology Tianjin 300384, P.R. China.

Experimental details

1. Synthesis

Single crystals of $Ba_8SrPb_{24}O_{24}Cl_{18}$ were grown through a high temperature solid state reaction. The mixtures of $BaCl_2$ (3 mmol, 0.625 g), $SrCl_2$ (1 mmol, 0.158 g) and PbO (10 mmol, 2.23 g) were put into a platinum crucible, heated up to 700 °C and held at this temperature for 48 h. Then the mixtures were cooled to 300 °C at a rate of 3 °C h^{-1} and cooled to room temperature by switching off the furnace. A light yellow block shaped crystal with dimensions of 0.1 × 0.1 × 0.2 mm^3 was selected for single crystal structure determination. Polycrystalline powder samples of $Ba_8SrPb_{24}O_{24}Cl_{18}$ were synthesized by a traditional solid state reaction with stoichiometric amounts of $BaCl_2$, $SrCl_2$ and PbO. The mixtures were ground, presintered at 200 °C for 12 h and heated to its sintering temperature of 480 °C. Pure powder samples of $Ba_8SrPb_{24}O_{24}Cl_{18}$ were obtained by maintaining this temperature for three days with several intermittent grindings.

2. Structure determination

Single crystal X−ray diffraction data were recorded on a Xcalibur Ecos diffractometer equipped with a graphite−monochromated Mo−K_α (λ = 0.71073 Å) radiation at 293 K. The structure was solved with direct method by SHELXS−97 and refined by the full matrix least squares on F^2 by SHELXL−97, respectively. The detailed crystallographic data were summarized in Table S1. The atomic coordinates, occupancy and equivalent displacement parameters are given in Table S2. The important bond lengths and angles are listed in Table S3.

3. Property Characterization

Powder X−ray Diffraction

The powder X−ray diffraction pattern of the as−obtained polycrystalline powder was performed at room temperature on a Bruker D8 Focus diffractometer with Cu K_α (λ = 1.5418 Å) radiation. The scanning step width of 0.1º and a fixed counting time 0.2 s/step were applied to record the patterns in the 2θ range of 10 – 70º.

Element Analysis

Elemental analysis of compositions of the single crystal was performed on an energy−dispersive X−ray (EDX)−equipped Hitachi S−4800 scanning electron microscopy (SEM) instrument.

Diffuse reflectance spectroscopy

A Cary 5000 UV−vis−NIR spectrophotometer with a diffuse reflectance accessory was used to measure the spectrum of $Ba_8SrPb_{24}O_{24}Cl_{18}$ and $BaSO_4$ (as a reference) in the range 276 nm (4.5 eV) to 2480 nm (0.5 eV).

Thermal Analysis

By applying the Labsys^{TM} TG−DTA16 (SETARAM) thermal analyzer equipped with the nitrogen flow at a rate of about 30 mL/min, the thermal stability of $Ba_8SrPb_{24}O_{24}Cl_{18}$ was investigated in detail. Appropriate amounts of the polycrystalline powder were thoroughly ground, then were placed in a silica tube (5 mm o.d. × 3 mm i.d.) and subsequently sealed under a high vacuum. The tube was heated from 298 to 1073 K and then cooled to room temperature with the heating/cooling rate both at 15 K min^{-1}.

4. Computational methods

The first–principles calculations for $Ba_8SrPb_{24}O_{24}Cl_{18}$ were performed by CASTEP, a plane–wave pseudopotential total energy package based density functional theory (DFT). The functional developed by Perdew–Burke–Emzerhoff (PBE) functional within the generalized gradient approximation (GGA) form were adopted to describe the exchange–correlation energy. The optimized norm–conserving pseudopotentials in the Kleinman–Bylander form for all the elements are used to model the effective interaction between atom cores and valence electrons. And Ba $5s^25p^66s^2$, Sr $4s^24p^65s^2$, Pb $5d^{10}6s^26p^2$, O $2s^22p^4$ and Cl $3s^23p^5$ electrons were treated as valence electrons, allowing the adoption of a relatively small basis set without compromising the computational accuracy. The high kinetic energy cutoff 600 eV and dense 1×1×2 Monkhorst–Pack k–point meshes in the Brillouin zones were chosen for $Ba_8SrPb_{24}O_{24}Cl_{18}$. Our tests showed that the above computational set ups are sufficiently accurate for present purposes. It is well known that the energy band gaps calculated by standard DFT method are smaller than the measured

values, due to the discontinuity of exchange–correlation energy. The scissor operators were adopted to shift all the conduction bands to match the calculated band gaps with the measured values. Based on the scissor–corrected electron band structure, the imaginary part of the dielectric function was calculated according to the electron transition from the valence bands (VB) to conduction band (CB). Consequently, the real part of the dielectric function is obtained by the Kramers–Kronig transform and the refractive index is determined.

5. Figure S1

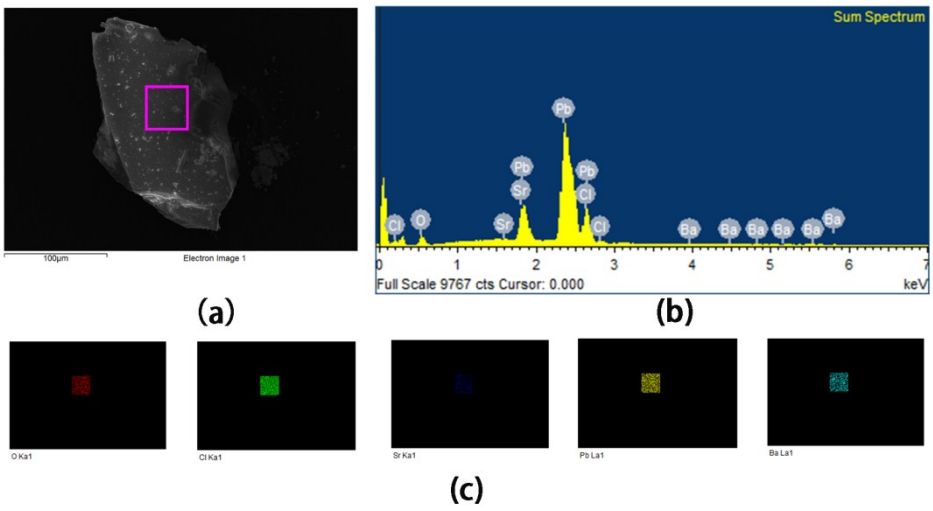

(a) Scanning electron microscopy (SEM) image of $Ba_8SrPb_{24}O_{24}Cl_{18}$; (b) Elemental analysis of $Ba_8SrPb_{24}O_{24}Cl_{18}$ by EDX spectroscopy. (c) Elemental distribution of the as-grown crystal (from left to right: O, Cl, Sr, Pb, Ba).

6. Figure S2

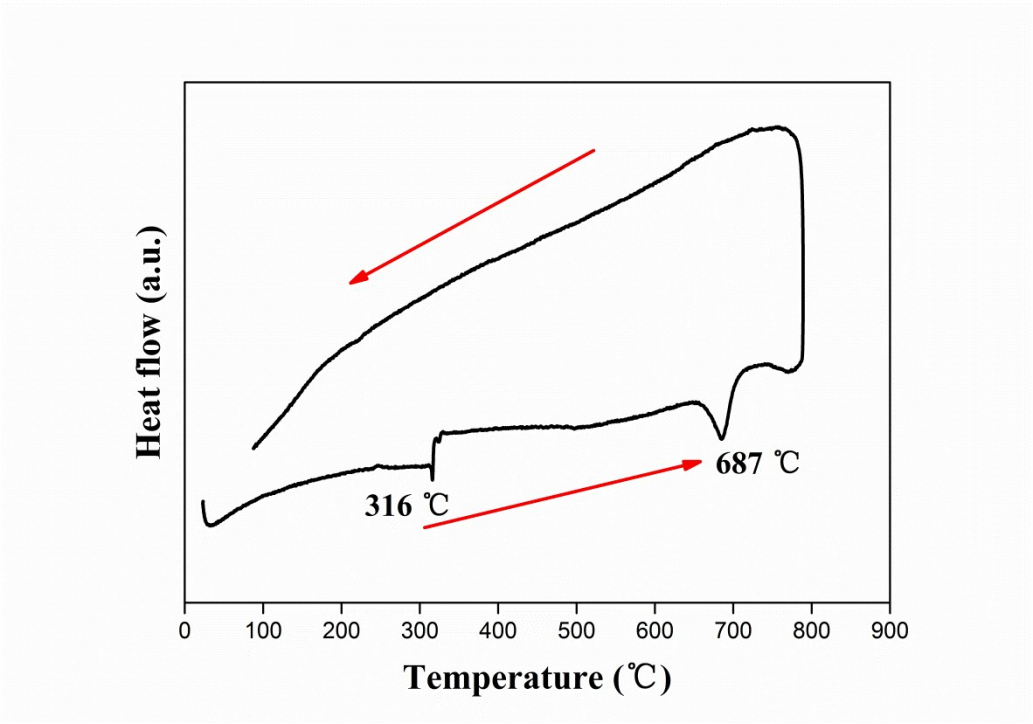

DSC curve of $Ba_8SrPb_{24}O_{24}Cl_{18}$

7. Table S1 Crystallographic data and structure refinement for $Ba_8SrPb_{24}O_{24}Cl_{18}$.

Empirical formula	$Ba_8SrPb_{24}O_{24}Cl_{18}$
Formula weight	2393.67
Space group	*I*4/*m*
a/Å	16.2418(4)
b/Å	16.2418(4)
c/Å	12.9864 (6)
α/°	90.00
β/°	90.00
γ/°	90.00
V/Å^3	3425.8 (2)
Z	6
ρ_{calc} g/cm^3	6.962
μ/mm^{-1}	64.744
F(000)	5904.0
Radiation	MoKα (λ = 0.71073 Å)
2*θ* range for data collection/°	6.274 to 52.74
Index ranges	$-20 \le h \le 20$, $-20 \le k \le 20$, $-15 \le l \le 16$
Reflections collected	24002
Independent reflections	1837 [R_{int} = 0.1205]

Data/restraints/parameters	1837/0/93
GOF on F^2	1.053
Final R indexes [I>=2σ (I)]	R_1 = 0.0354, wR_2 = 0.0866
Final R indexes [all data]	R_1 = 0.0401, wR_2 = 0.0894

8. Table S2 Fractional atomic coordinates ($\times 10^4$) and equivalent isotropic displacement parameters ($Å^2 \times 10^3$) for $Ba_8SrPb_{24}O_{24}Cl_{18}$. U_{eq} is defined as 1/3 of of the trace of the orthogonalized U_{ij} tensor.

Atom	x	y	z	Wyckoffsite	U(eq)
Pb3	8522.9(2)	9021.7(3)	3513.8(3)	16i	14.62(15)
Pb1	10232.7(2)	6286.8(3)	3562.1(3)	16i	14.25(15)
Pb2	9373.4(2)	7462.5(3)	1543.1(3)	16i	16.45(15)
Ba1	7911.5(4)	6692.6(4)	3432.3(6)	16i	19.8(2)
Sr1	5000	5000	5000	2a	15.6(5)
Cl1	9278(3)	7578(3)	5000	8h	26.0(9)
Cl3	7247(3)	8248(3)	5000	8h	27.3(9)
Cl4	6521(3)	5942(3)	5000	8h	36.6(12)
Cl2	8718(3)	5406(3)	5000	8h	32.8(11)
Cl5	5000	5000	2793(5)	4e	54(2)
O1	9155(4)	6287(4)	2464(5)	16i	13.6(15)
O2	8343(4)	7953(4)	2570(5)	16i	15.6(16)
O3	7485(4)	9534(4)	2659(5)	16i	13.4(14)

9. Table S3 Selected bond lengths (Å) and angles (°) for $Ba_8SrPb_{24}O_{24}Cl_{18}$.

Pb1−O1$^{\#2}$	2.286(7)	O1−Pb1−O1$^{\#2}$	102.3(2)
Pb3−O2	2.145(7)	O2−Pb3−O3	85.0(3)
Pb3−O3	2.184(7)	O1$^{\#2}$−Pb1−O3$^{\#3}$	81.1(3)
Pb1−O1	2.257(7)	O1−Pb1−O3$^{\#3}$	78.8(2)
Pb1−O3$^{\#3}$	2.303(7)	O1−Pb2−O2	82.6(2)
Pb2−O1	2.281(7)	O1−Pb2−O3$^{\#3}$	78.6(2)
Pb2−O2	2.283(7)	O2−Pb2−O3$^{\#3}$	101.1(3)
Pb2−O3	2.291(7)		

10. Table S4 Structure characteristics of related Pb-containing oxyhalides.

Compound	Space group	Structure characteristics	Fundamental building blocks
$Pb_3O_2Br_2$	*Pnma*	1D infinite chain	PbO_2, PbO_4
$Pb_3O_2Cl_2$	*Pnma*	1D infinite chain	PbO_2, PbO_4
$Pb_{13}O_{10}Br_6$	*C*2/*c*	3D crisscross network	PbO_2, PbO_3, PbO_4
$Pb_{13}O_{10}Cl_6$	*C*2/*c*	3D crisscross network	PbO_2, PbO_3, PbO_4
$Pb_9O_4Br_{10}$	*P*4/*n*	0D isolated [Pb_8O_4] units	PbO, PbO_3
$Pb_{2.16}OCl_{2.32}$	*Fm*2*m*	1D infinite chain	PbO_2

$Pb_{17}O_8Cl_{18}$	*Fmm*2	1D infinite chain	PbO_2
$Pb_4O_4Cl_2$	*I*4/*mmm*	2D Pb−O layer	PbO_4
$Pb_7O_8Cl_2$	*I*4/*mmm*	2D Pb−O layer	PbO_4